Journal of Autoimmunity 81 (2017) 56–67

Contents lists available at ScienceDirect

Journal of Autoimmunity

journal homepage: www.elsevier.com/locate/jautimm

Central immune tolerance depends on crosstalk between the classical and alternative NF-κB pathways in medullary thymic epithelial cells

Marc Riemann [a, *], Nico Andreas [a], Maria Fedoseeva [a], Elke Meier [a], Debra Weih [a], Helga Freytag [a], Ruth Schmidt-Ullrich [b], Ulf Klein [c, 1], Zhao-Qi Wang [d], Falk Weih [a, 2]

[a] Research Group Immunology, Leibniz Institute on Aging – Fritz Lipmann Institute, 07745 Jena, Germany
[b] Signal Transduction Laboratory, Max Delbrück Center for Molecular Medicine, 13125 Berlin, Germany
[c] Herbert Irving Comprehensive Cancer Center, Departments of Pathology & Cell Biology and Microbiology & Immunology, Columbia University, New York, NY 10032, USA
[d] Research Group Genomic Stability, Leibniz Institute on Aging – Fritz Lipmann Institute, 07745 Jena, Germany

ARTICLE INFO

Article history:
Received 16 December 2016
Received in revised form
13 March 2017
Accepted 13 March 2017
Available online 3 April 2017

Keywords:
Autoimmunity
Central immune tolerance
Medullary thymic epithelial cells
NF-κB
Conditional gene targeting

ABSTRACT

Medullary thymic epithelial cells (mTECs) contribute to self-tolerance by expressing and presenting peripheral tissue antigens for negative selection of autoreactive T cells and differentiation of natural regulatory T cells. The molecular control of mTEC development remains incompletely understood. We here demonstrate by TEC-specific gene manipulation in mice that the NF-κB transcription factor subunit RelB, which is activated by the alternative NF-κB pathway, regulates development of mature mTECs in a dose-dependent manner. Mice with conditional deletion of *Relb* lacked mature mTECs and developed spontaneous autoimmunity. In addition, the NF-κB subunits RelA and c-Rel, which are both activated by classical NF-κB signaling, were jointly required for mTEC differentiation by directly regulating the transcription of *Relb*. Our data reveal a crosstalk mechanism between classical and alternative NF-κB pathways that tightly controls the development of mature mTECs to ensure self-tolerance.

1. Introduction

Most T lymphocytes develop in the thymus, consisting of the outer cortex and the inner medulla. In the cortex T cell progenitors with random α/β T cell receptor specificities are generated, including cells recognizing self-antigens. In the thymic medulla most autoreactive T cells are either deleted by apoptosis (negative selection) or they differentiate into natural regulatory T cells (nTregs). Both mechanisms contribute to the establishment of self-tolerance and require the recognition of self-antigen/MHC complexes displayed on antigen-presenting cells (APCs) [1]. Medullary thymic epithelial cells (mTECs), which are the major stromal component of the medulla, can act as APCs, and are the main source for non-ubiquitous peripheral tissue antigens (PTAs) in the thymus [2]. Expression of numerous PTAs, such as insulin-2 and salivary protein-1 by mature mTECs is dependent on the transcription factor Aire, and mutations in the *Aire* gene can lead to autoimmunity in mice and men [3]. In addition, dendritic cells (DCs) transport self-antigens from the periphery into the thymus and are involved in self-tolerization [4,5]. Both mTECs and DCs are able to delete self-reactive T cells and induce Treg cells, creating two distinct T cell pools with divergent TCR repertoires via both tolerization modes [6]. Furthermore, presentation of mTEC-derived self-antigens by DCs plays an important role in tolerance induction.

mTECs and cortical TECs (cTECs) have been postulated to derive from a bipotent epithelial progenitor [7]. However, recently it has been suggested that mTECs do not derive from a lineage-negative progenitor but rather from precursors expressing hallmarks of cTECs, such as CD205 and the thymoproteasome subunit β5t [8,9]. Furthermore, downstream of a common TEC progenitor a lineage-restricted mTEC stem cell seems to exist, which gives lifelong rise to $CD80^{lo}MHCII^{lo}$ immature and $CD80^{hi}MHCII^{hi}$ mature mTECs [10]. Dependent on LTβR signaling mature mTECs can further progress into post-Aire stages, which are $CD80^{lo}MHCII^{lo}$ again. Terminally differentiated $Aire^{-}$ mTECs have high expression of involucrin and

* Corresponding author. Immunology Group, Leibniz Institute on Aging – Fritz Lipmann Institute, Beutenbergstrasse 11, 07745 Jena, Germany.
E-mail address: marc.riemann@leibniz-fli.de (M. Riemann).
[1] The present address is Experimental Haematology, Leeds Institute of Cancer and Pathology, University of Leeds, Leeds LS9 7TF, United Kingdom.
[2] Deceased.

http://dx.doi.org/10.1016/j.jaut.2017.03.007

form Hassals' corpuscle-like structures in mouse thymus [11]. Lymphoid tissue inducer cells and Vγ5$^+$ γδ T cells in the embryo as well as *i*NKT cells and positively selected CD4 single-positive thymocytes in adult mice have been shown to induce commitment and maturation of the mTEC lineage [12–15]. This occurs via activation of the TNF receptor superfamily members RANK, CD40, and LTβR, which can trigger both the classical and the alternative NF-κB pathways [12,16–18].

In vertebrates the NF-κB/Rel transcription factor family comprises five members, RelA (p65), RelB, c-Rel, p50 (NF-κB1) and p52 (NF-κB2), which form different homo- and heterodimers. In resting cells the dimers are kept in the cytoplasm by interaction with inhibitory IκB proteins [17]. The classical NF-κB pathway can be induced by many different stimuli, such as TNF, IL-1β or LPS. Via activation of IKKβ it leads to phosphorylation and degradation of IκBα, and the nuclear translocation of RelA/p50 and c-Rel/p50 heterodimers [17]. In contrast, the alternative NF-κB pathway is only activated together with the classical pathway by a few members of the TNFR superfamily, such as RANK, CD40 and LTβR. The signaling occurs via NIK and IKKα, leads to the processing of the inhibitory NF-κB2 precursor p100 and culminates in the activation of RelB/p52 complexes [17].

Alternative NF-κB signaling has been shown to play a major role in mTEC differentiation. Mice deficient for components of this pathway have a reduction in mTEC numbers and develop autoimmune syndromes [19–24]. However, systemic inactivation of alternative NF-κB signaling also leads to defects in the development of secondary lymphoid organs and DCs, which might contribute to the autoimmune phenotypes in these mice [25,26]. Indeed, mice with TEC-specific ablation of *Traf6*, which exclusively lack mTECs, develop only a rather mild autoimmune hepatitis [27].

Traf6, which binds to the intracellular domains of RANK and CD40, has been shown to play a role in multiple signaling pathways [28]. However, it is not involved in alternative NF-κB signaling, indicating that an unknown pathway downstream of Traf6 is essential for mTEC differentiation. Although classical NF-κB signaling can be transduced by Traf6, its implication in mTEC differentiation has not yet been genetically investigated.

We show here that mTEC development is critically dependent on the activation of RelA and c-Rel via the classical NF-κB pathway. Both factors transcriptionally regulate the expression level of RelB, which determines the total number of mTECs per thymus in a dose-dependent manner. Complete absence of mature mTECs by TEC-specific inactivation of *Relb* results in symptoms of systemic autoimmunity. All together, these results show that the crosstalk between both NF-κB pathways culminating in the activation of a high amount of RelB protein is important for the development of sufficient mTECs to guarantee the establishment of self-tolerance.

2. Materials and methods

2.1. Mice

Foxn1-Cre [29], *Rela^{flox}* [30], *c-Rel^{flox}* [31], *Traf6^{flox}* [32] and *κB-EGFP* [33] mice have been described previously. *Generation of Relb^{flox} mice:* To construct the targeting vector a floxed *neomycin* (*neo*) resistance cassette was cloned into the AscI site of the 4th intron of the *Relb* gene (Supplemental Fig. 1). A single *loxP* site was placed into the BglII site 184 bp upstream of exon 4. The length of the homologous sequence upstream of the 5′ *loxP* site was 2.75 kb. The HSV *thymidine kinase* gene was inserted 0.8 kb downstream of the *neo* cassette for selection against random integration events. E14.1 embryonic stem (ES) cells that were cultured in ES medium (DMEM, 15% FCS, 1× sodium pyruvate, 1× Pen/Strep, 1× L-glutamine, 1× non-essential amino acids, 1 μM 2-mercaptoethanol, 1000 units/ml LIF (ESGRO®; Chemicon) were electroporated with the linearized targeting vector and selected with G418 (200 μg/ml; Invitrogen) and gancyclovir (Cyméven; 2 μM; Roche). Resistant clones were screened for homologous recombination by Southern blot analysis of BamHI-digested genomic DNA using an external 3'-flanking probe. Positive clones were further analyzed by Southern blotting using a *neo* probe to exclude clones with additional random integrations of the targeting construct in the genome. The *neo* cassette was deleted by transient transfection of a plasmid (*pMC-cre*) expressing Cre recombinase. Clones containing the floxed allele were identified by Southern blots of BamHI/HindIII-digested genomic DNA and PCR. The presence of *loxP* sites was verified by sequencing. Properly targeted ES cell clones were injected into C57BL/6 blastocysts and chimeric mice were tested for germline transmission of the *Relb^{flox}* allele. *Generation of Rosa26-Relb transgenic mice:* For targeting the *Relb* transgene into the *Rosa26* locus we used the TV-Rosa26 vector (kindly provided by U. Zimber-Strobl, Helmholtz Zentrum München) containing a *loxP*-flanked stop cassette with a transcription and translation termination site (Supplemental Fig. 2). A murine *Relb* cDNA was inserted downstream of the stop cassette. The linearized targeting vector was electroporated into E14.1 ES cells. G418 resistant clones were screened for homologous recombination by Southern blot analysis of EcoRI-digested genomic DNA using an external 5'-flanking probe. Targeted ES cells were injected into C57BL/6 blastocysts to obtain chimeric mice, which were backcrossed with C57BL/6 mice to obtain germline transmission of the *Relb* transgene. *Generation of Relb-Cre-P2A-Katushka mice:* Generation of the BAC transgenic mice was performed by PolyGene (Switzerland). A BAC of 93 kb (bMQ-258k08) containing the complete *Relb* locus with 45 kb of upstream region was modified by introducing the gene coding for a Cre-P2A-Katushka fusion protein into the first exon of the *Relb* gene (Supplemental Fig. 3). The construct was injected into pronuclei from fertilized C57BL/6 oocytes and four founder mice were obtained, which transmitted the transgene to the progeny. In one of these founder lines (#53) transgene expression nicely reflected that of endogenous *Relb* (Riemann et al., manuscript in preparation).

All mouse lines were on a C57BL/6J background. The mice were analyzed at the age of 4–6 weeks unless otherwise indicated. Floxed littermates without *Foxn1-Cre* transgene were used as controls since analysis of the pure *Foxn1-Cre* mice did not show any significant alterations in the thymus. All experiments were performed in accordance with the ethic committee guidelines.

2.2. Histology and immunohistochemistry

Tissues were fixed in 10% buffered formalin, embedded in paraffin blocks, sectioned at 6 μm, and stained with hematoxylin and eosin (H&E). For immunohistochemistry, thymi were embedded in Neg-50 frozen section medium (Richard Allen Scientific) and frozen on dry ice. Ten μm thick sections were cut, air-dried, and fixed in cold acetone. Staining was performed either with biotinylated *Ulex europaeus* agglutinin-1 (UEA-1) (Vector Laboratories) or with antibodies against Aire (M-300; Santa Cruz), claudin-3 and -4 (Zymed), keratin-5 (Covance), or RelB (C-19; Santa Cruz) followed by biotinylated anti-rabbit IgG (Vector Laboratories). Staining with MIDC8 antibody (Antikoerper-online) was followed by biotinylated anti-rat IgG (Vector Laboratories). All sections were then incubated with Vectastain ABC peroxidase (Vector Laboratories). Diaminobenzidine was used to visualize the immunostaining and counterstaining was performed with Mayer's hematoxylin. All sections were examined by light microscopy using an Olympus BX41 microscope.

2.3. Flow cytometry and sorting of thymic epithelial cells

Single-cell suspensions of thymic stromal cells were prepared in 5 digestion steps with collagenase D, dispase, and DNase I (Roche) as described [34]. For TEC analysis, cells were stained with anti-CD45-PE-Cy7 (clone 30-F11), anti-EpCAM-PE (G8.8), anti-Ly51(BP1)-FITC/Biotin (6C3), and anti-CD80-APC/PerCP-Cy5.5 (BD) (16-10A1). Streptavidin-PerCP-Cy5.5 was used as secondary reagent. For intracellular staining with anti-Aire-AF647 (5H12), anti-c-Rel-PE (1RELAH5), anti-Ki67-FITC (B56), or anti-cleaved caspase-3 (Asp175; Cell Signaling) followed by anti-rabbit-IgG-Pacific Blue (Invitrogen), cells were fixed and stained using FoxP3 fixation and permeabilization kit (eBioscience). Analyses were performed with a FACSCanto II (BD). For TEC sorting, stromal cells were enriched by depletion of $CD45^+$ cells using a magnetic cell sorter (Miltenyi Biotec) prior to sorting with a FACSAria II (BD). Antibodies were obtained from eBioscience unless otherwise stated.

2.4. Flow cytometry of infiltrating cells in lung and liver

For isolation of infiltrating cells, lung tissues were digested for 1 h with collagenase IV-S (Sigma). Liver tissues were minced by pressing through a metal sieve and subsequently suspended by several passages through a 21-gauge needle. Suspensions of both tissues were filtered through 40 μm cell strainers and purified using Percoll density gradients. Red blood cells were depleted with ACK lysis buffer (150 mM NH_4Cl, 10 mM $KHCO_3$, 0.1 mM EDTA, pH 7.3). Single-cell suspensions were stained with anti-TCRβ-PerCP-Cy5.5 (H57-597), anti-CD4-PE (GK1.5), anti-CD8α-eFluor450 (53−6.7), anti-CD62L-FITC (MEL-14), and anti-CD44-APC (IM7) (all antibodies from eBioscience). Analyses were performed with a FACSCanto II (BD).

2.5. Flow cytometry of thymic DCs and T cells

Thymi were minced with scissors into small pieces and digested with collagenase D and DNase I (Roche). After erythrocyte lysis in ACK buffer (see above) cells were filtered through a 40 μm cell strainer. DCs were stained with anti-CD11c-APC (N418), anti-SIRPα (CD172a)-Biotin (P84) followed by Streptavidin-PE and anti-PDCA1-FITC (eBio927). For T cell analysis staining was performed with anti-TCRβ-PerCP-Cy5.5 (H57-597), anti-TCRγδ-PE (eBioGL3), anti-CD4-PE-Cy7 (BD) (RM4-5), anti-CD8α-EF450/PE-Cy7/APC-H7 (BD) (53−6.7) antibodies and αGalCer-CD1d-PE tetramer (NIH tetramer core facility). For intracellular staining with anti-FoxP3-PE cells were fixed and stained using FoxP3 fixation and permeabilization kit (eBioscience). Analysis was performed with a FACSCanto II (BD).

2.6. Quantitative real-time RT-PCR (qRT-PCR)

Total RNA was isolated from thymi or sorted mTECs using the RNeasy Minikit (Qiagen) or the RNAqueous-Micro kit (Ambion), respectively. First-strand cDNA synthesis was conducted with 1 μg of RNA using oligo$(dT)_{12\text{-}18}$ primer and M-MLV reverse transcriptase (H-) (Promega). For relative quantification of mRNA, amplification of sample cDNA was monitored with an iCycler (Bio-Rad) using the fluorescent DNA-binding dye SYBR Green (Bioline). Target mRNA levels in each sample were normalized to the endogenous *Actb* mRNA levels. The primers used were as follows: *Csna*, 5′-GACTGAGCCAGTCCTACTATCCACATA-3′ and 5′-GAAAGGCA-TCA-TACTGGAAGATTTG-3′; *Sp1*, 5′-TGGTGTTTCCACTATCCTAGTCTCTTG-3′ and 5′-CGACTGAATCAGAGGAATCAACTTC-3′; *Ins2*, 5′-GCCTATCTT CCAGGTT-ATTGTTTCAA-3′ and 5′-TCCCCACACACCAGGTAGAGA-3′; *Crp*, 5′-TTTTAGCCC-CAGCAGATGTTGT-3′ and 5′-TAAGTCAGATTCT CTTTGGTAGAGTCCTAGT-3′; *Fabp9*, 5′-GAATGTGAGCCCCGGAAAGT-3′ and 5′-TCTGCAGTGGTCTCTTCAAA-TTCT-3′; *Relb*, 5′-GTGACCTCT CTTCCCTGTCACTAAC-3′ and 5′-CAGCGTGACG-CTGCTCAGT-3′; *Nfkb2*, 5′-GCTAATGTGAATGCCCGGAC-3′ and 5′-CTTTGGGTA-TCCC TCTCAGGC-3′; *Actb*, 5′-TGGCGCTTTTGACTCAGGA-3′ and 5′-GGG AGGG-TGAGGGACTTCC-3′.

2.7. Western blots

Liver tissue from *Rag1*$^{-/-}$ mice was homogenized in lysis buffer (20 mMTris-HCl pH 8.8, 10 mM NaCl, 1 mM EDTA, 0.5% NP-40, 0.1% SDS, protease inhibitor cocktail from Roche) and lysates were centrifuged for 5 min at 16,100 g. Supernatants were mixed 1/1 with sample buffer (250 mM Tris-HCl pH 6.8, 2% SDS, 10% glycerol, 20 mM DTT, 0.01% bromophenol blue), 10 μg of protein per lane were separated by SDS-PAGE (10%), and electroblotted onto Immobilon P membranes (Millipore). Membranes were blocked with 5% non-fat milk-TBST (10 mM Tris-HCl pH 8.0, 150 mM NaCl, 0.2% Tween 20) for 2 h and incubated with sera from individual mice diluted 1/200 in 5% non-fat milk-TBST overnight. After three washes with TBST, membranes were incubated with HRP-conjugated goat-anti-mouse IgG (1:10,000; Dako) in TBST for 2 h and washed 3 times with TBST. Immuno-reactive proteins were detected using an ECL visualization system (GE Healthcare).

2.8. Western blots of 3T3 mouse embryonic fibroblasts (MEFs)

For activation of classical NF-κB 3T3 MEFs were stimulated with TNF (10 ng/ml; Sigma-Aldrich). For preparation of whole-cell protein extracts the cells were homogenized in lysis buffer (50 mM Hepes pH 7.9, 150 mM NaCl, 1 mM EDTA, 0.5% NP-40, 10% glycerol, protease inhibitor cocktail from Roche) and centrifuged for 10 min at 16,100 g. The supernatants were mixed 1/1 with sample buffer and Western blots were performed as described in *Western blots*. Nuclear extracts were prepared as previously described [35]. For immunoprecipitation whole-cell extract was incubated with anti-IκBα-antibody-coupled agarose beads (Santa Cruz) at 4 °C over night. The beads were washed three times with PBS and incubated in sample buffer at 95 °C for 5 min to elute precipitated proteins. After centrifugation at 1000 g the supernatant was analyzed by Western blot. Antibodies specific for RelA (C-20; 1:1000), c-Rel (C; 1:500), RelB (C-19; 1:1000), β-Actin (I-19; 1:1000), c-Jun (N; 1:1000) and IκBα (C-21; 1:1000) from Santa Cruz were used as primary and HRP-conjugated goat-anti-rabbit or rabbit-anti-goat IgG (Dako; 1:2000) were used as secondary antibodies.

2.9. Chromatin immunoprecipitation (ChIP)

In vivo binding of NF-κB subunits to the *Relb* promoter in 3T3 MEFs was analyzed by chromatin immunoprecipitation using the “ChIP-IT Express Enzymatic” Magnetic Chromatin Immunoprecipitation Kit (Active Motif). The ChIP was carried out according to the manufacturer's instructions using 5 μg chromatin enzymatically sheared for 6 min and 3 μg antibody (α-RelA (C-20), α-c-Rel (C), and α-RelB (C-19); all from Santa Cruz). One-twentieth of the DNA was used in each PCR reaction (40 cycles) applying the following primers for the *Relb* promoter (−440/-293), sense, 5′-CTTGTTCTGTGGGTAGGGCG-3′, antisense, 5′-CCGCTGCTCACGT-GACT-3′. 10 ng DNA of input-chromatin was applied in control PCR reactions.

2.10. Statistical analysis

Results are depicted as mean values ± SD. Statistical analysis was performed using Student's two-tailed unpaired *t*-test for

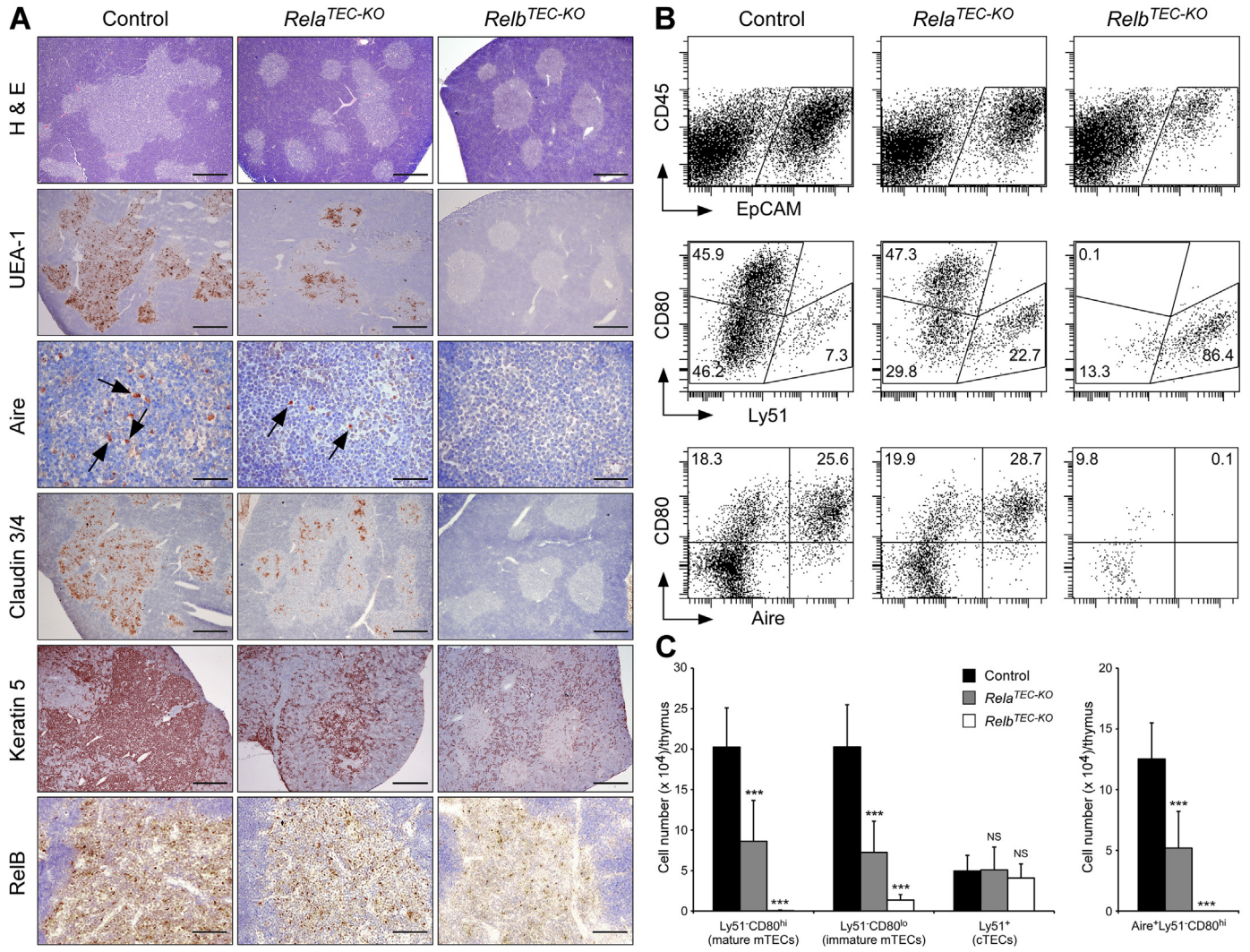

Fig. 1. Both RelA and RelB are required for proper development of mTECs. (A) Thymus sections from control, *Rela*$^{TEC\text{-}KO}$, and *Relb*$^{TEC\text{-}KO}$ mice were stained with H&E, UEA-1, or antibodies against Aire, claudin 3 and 4, keratin 5, or RelB. Scale bars: 50 μm (Aire), 100 μm (RelB), or 500 μm. (B) Thymus single-cell suspensions were stained with antibodies against CD45, EpCAM, Ly51, and CD80 and analyzed by flow cytometry. CD45$^-$EpCAM$^+$ TECs (upper row) were segregated into Ly51$^-$CD80^{hi} mature mTECs, Ly51$^-$CD80^{lo} immature mTECs, and Ly51$^+$CD80^{lo} cTECs (middle row). Aire expression was analyzed by intracellular staining (lower row). Numbers in the respective gates indicate frequencies of cells within each TEC subpopulation. (C) Quantitative summary of total cell numbers of indicated TEC subpopulations per thymus from control (n = 10), *Rela*$^{TEC\text{-}KO}$ (n = 8), and *Relb*$^{TEC\text{-}KO}$ (n = 4) mice. Data represent mean values ± SD.

comparisons between two groups with unequal variances. Differences were considered significant at $^*P < 0.05$; $^{**}P < 0.01$; $^{***}P < 0.001$; NS, not significant.

3. Results

3.1. Both RelA and RelB are required for proper development of mTECs

Systemic *Relb*$^{-/-}$ mice lack mature mTECs and develop a severe autoimmune syndrome with inflammatory infiltrates in multiple organs [19,20]. To investigate whether TEC-specific deletion of RelB is sufficient to ablate mTECs resulting in severe autoimmunity, we generated *Relb*^{flox} mice and crossed them with *Foxn1-Cre* mice to obtain conditional *Relb*$^{TEC\text{-}KO}$ mice. In addition, we generated *Rela*$^{TEC\text{-}KO}$ mice to investigate the role of the classical NF-κB pathway in mTEC development and the establishment of self-tolerance.

In contrast to *Relb*$^{-/-}$ mice, which exhibit severe thymic atrophy predominantly affecting the medulla [20], both *Rela*$^{TEC\text{-}KO}$ and *Relb*$^{TEC\text{-}KO}$ mice displayed only a minor reduction of medullary areas in H&E stained sections (Fig. 1A). However, *Relb*$^{TEC\text{-}KO}$ mice completely lacked mature UEA-1$^+$ and Aire$^+$ mTECs while they were partially reduced and unevenly distributed in *Rela*$^{TEC\text{-}KO}$ thymi. Keratin 5 staining confirmed the absence of TECs in medullary areas of *Relb*$^{TEC\text{-}KO}$ mice, whereas they were only partially reduced in *Rela*$^{TEC\text{-}KO}$ mice. Claudin-3 and -4 (Cld3,4) are expressed already by early precursors of mature Aire$^+$ mTECs [36]. Thus, the absence of Cld3,4$^+$ cells in *Relb*$^{TEC\text{-}KO}$ thymi indicated that mTEC differentiation was blocked at an early maturation stage. Cld3,4$^+$ cells were also reduced in *Rela*$^{TEC\text{-}KO}$ thymi, although less pronounced. We next quantified immature and mature subpopulations among total mTECs by flow cytometry. For detection of these cells we used antibodies against the following markers: (1) CD45, which is highly expressed on hematopoietic, but not on stromal cells, (2) EpCAM, which is specifically expressed on all thymic epithelial cells, (3) Ly51, which is expressed on cTECs but not on mTECs and (4) CD80, which shows high expression on mature mTECs (13).

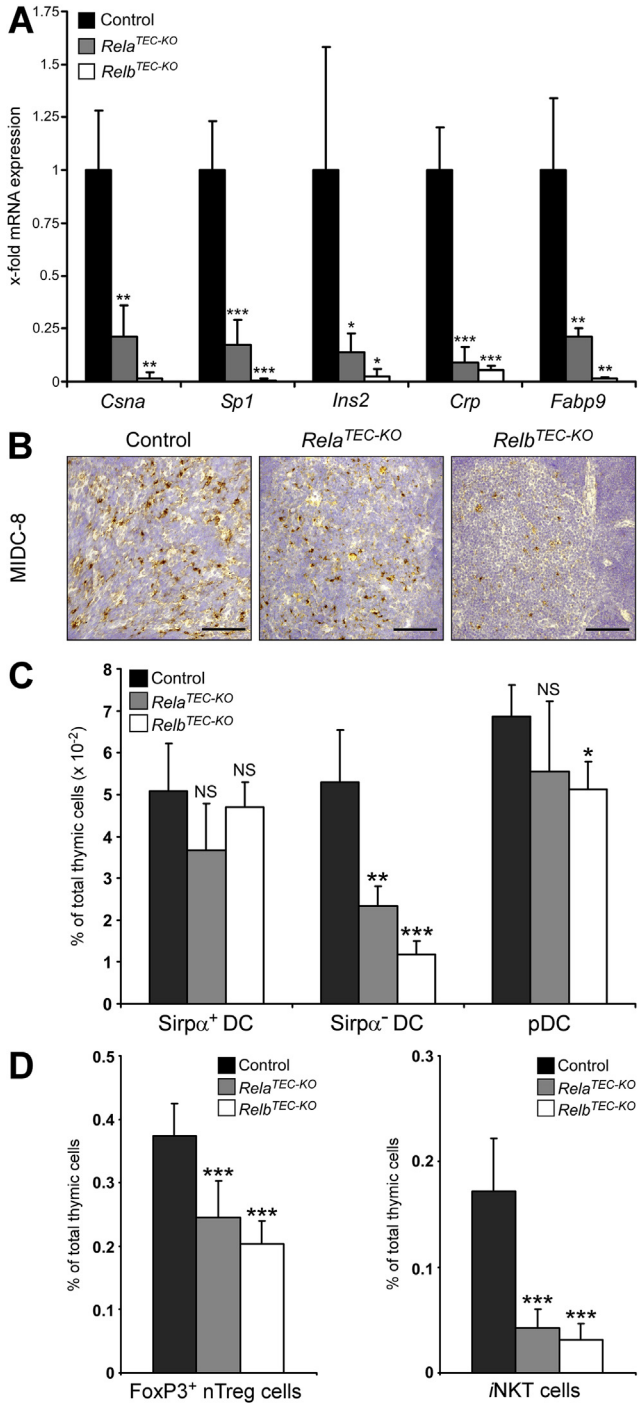

Fig. 2. Loss of mTECs affects PTA expression as well as cell numbers of thymic DCs, nTregs, and *i*NKT cells. (A) mRNA levels of Aire-dependent (*Csna*, *Sp1*, *Ins2*) and Aire-independent PTAs (*Crp*, *Fabp9*) were determined by qRT-PCR of control, $Rela^{TEC\text{-}KO}$, and $Relb^{TEC\text{-}KO}$ thymi (n = 3–6). Data represent mean values ± SD relative to control values after normalization to *Actb*. (B) Thymus sections from control, $Rela^{TEC\text{-}KO}$, and $Relb^{TEC\text{-}KO}$ mice were stained with MIDC-8 antibody to detect DCs. Scale bars represent 100 μm. (C) Proportions of the three major DC subpopulations in control (n = 6), $Rela^{TEC\text{-}KO}$ (n = 3), and $Relb^{TEC\text{-}KO}$ (n = 3) thymi. Thymus single-cell suspensions were stained with antibodies against CD11c, Sirpα, and PDCA1 for flow cytometry. Cells were classified into $CD11c^{high}Sirp\alpha^{+}$/$Sirp\alpha^{-}$ cDCs and $CD11c^{int}PDCA1^{+}$ pDCs. (D) Proportions of $CD4^{+}CD8^{-}FoxP3^{+}$ nTregs and $TCR\beta^{int}V\alpha14J\alpha18^{+}$ *i*NKT cells among total thymocytes from control (n(nTregs) = 14; n(*i*NKT) = 10), $Rela^{TEC\text{-}KO}$ (n(nTregs) = 8; n(*i*NKT) = 5), and $Relb^{TEC\text{-}KO}$ (n(nTregs) = 6; n(*i*NKT) = 5) mice. Data represent mean values ± SD.

Whereas $Relb^{TEC\text{-}KO}$ thymi completely lacked mature ($CD80^{hi}$) and had dramatically decreased numbers of immature ($CD80^{lo}$) mTECs (Fig. 1B and C), both mTEC populations were only 2.5-fold reduced in $Rela^{TEC\text{-}KO}$ thymi. Remaining mTECs showed complete deletion of the floxed *Rela* allele (Supplemental Fig. 4), indicating that loss of RelA affected mTEC development also at an early stage. This notion was further supported by normal proliferation and apoptosis rates in the remaining mTECs from $Rela^{TEC\text{-}KO}$ mice (Supplemental Fig. 5). The transcription factor Aire is expressed in 50–60% of mature $CD80^{hi}$ mTECs [34]. To evaluate whether RelA was involved in the generation of $Aire^{+}$ mTECs, we analyzed intracellular Aire expression. Absolute numbers of $Aire^{+}$ mature mTECs were clearly reduced in $Rela^{TEC\text{-}KO}$ mice, but the proportion within the mature mTEC subpopulation was unaltered (Fig. 1B and C). $Relb^{TEC\text{-}KO}$ mice did not contain any $Aire^{+}$ mTECs. Importantly, numbers of $CD45^{-}EpCAM^{+}Ly51^{+}$ cTECs were unchanged in both mutant mouse lines demonstrating that RelA and RelB specifically regulated the differentiation of mTECs. This corresponded to the restriction of RelB expression to the medulla (Fig. 1A). Collectively, these results show that both RelA and RelB regulate the development of mature mTECs. However, while the function of RelB is essential, the absence of RelA only affects the quantity of apparently unimpaired mTECs.

3.2. Loss of mTECs affects PTA expression as well as cell numbers of thymic DCs, nTregs, and iNKT cells

mTECs have been implicated in the establishment of immunological self-tolerance due to their capability to express and present a wide range of PTAs, which drives both negative selection as well as differentiation of nTregs [1]. In agreement with the complete lack of $Aire^{+}$ mTECs in $Relb^{TEC\text{-}KO}$ thymi, mRNA expression of the Aire-dependent PTAs casein-α, salivary protein-1, and insulin-2 was strongly decreased compared to control thymi (Fig. 2A). While expression of the Aire-independent PTA Fabp-9 was also almost absent, the mRNA encoding C-reactive protein was slightly higher expressed, which is in agreement with low level expression of this PTA in cTECs [2]. In contrast, $Rela^{TEC\text{-}KO}$ thymi expressed PTAs at reduced but higher levels than $Relb^{TEC\text{-}KO}$ thymi. However, the reduction in PTA expression was more pronounced than the decrease of mTEC numbers, suggesting that RelA may also be involved in the regulation of PTA expression itself. Besides mTECs, DCs are involved in the induction of central tolerance in the thymus [1]. $SIRP\alpha^{+}$ conventional DCs (cDCs) as well as $PDCA1^{+}$ plasmacytoid DCs (pDCs) have been shown to transport self-antigens from the periphery to the thymus where the antigens are presented for negative selection of autoreactive T cells and differentiation of nTregs [5]. Furthermore, $SIRP\alpha^{-}$ cDCs, which develop in the thymus, are involved in negative selection by cross-presentation of mTEC-derived antigens to $CD8^{+}$ T cells [37]. Immunohistochemical analysis of thymus sections using MIDC-8 antibody revealed markedly reduced DC staining in $Relb^{TEC\text{-}KO}$ mice (Fig. 2B). $Rela^{TEC\text{-}KO}$ mice had only slightly reduced numbers of DCs, which were not evenly distributed in the medulla, reminiscent of the distribution of $UEA\text{-}1^{+}$ mTECs in $Rela^{TEC-KO}$ thymus. Flow cytometric analysis of the three DC subpopulations revealed a specific loss of thymic $SIRP\alpha^{-}$ cDCs in $Relb^{TEC\text{-}KO}$ mice (Fig. 2C). In contrast, the percentage of $SIRP\alpha^{+}$ cDCs was not affected and pDCs were only slightly decreased in the absence of mature mTECs. The proportion of $SIRP\alpha^{-}$ cDCs was also diminished in $Rela^{TEC\text{-}KO}$ thymi, while $SIRP\alpha^{+}$ cDCs and pDCs were not affected. These results indicated that development and/or localization of $SIRP\alpha^{-}$ cDCs in the thymus is dependent on the presence of mTECs.

Analysis of different T cell subpopulations showed normal frequencies of CD4 and CD8 single-positive αβ T cells and of γδ T cells in both $Rela^{TEC\text{-}KO}$ and $Relb^{TEC\text{-}KO}$ mice (Supplemental Fig. 6). However, both mouse lines had a significant reduction of $FoxP3^{+}$ nTregs,

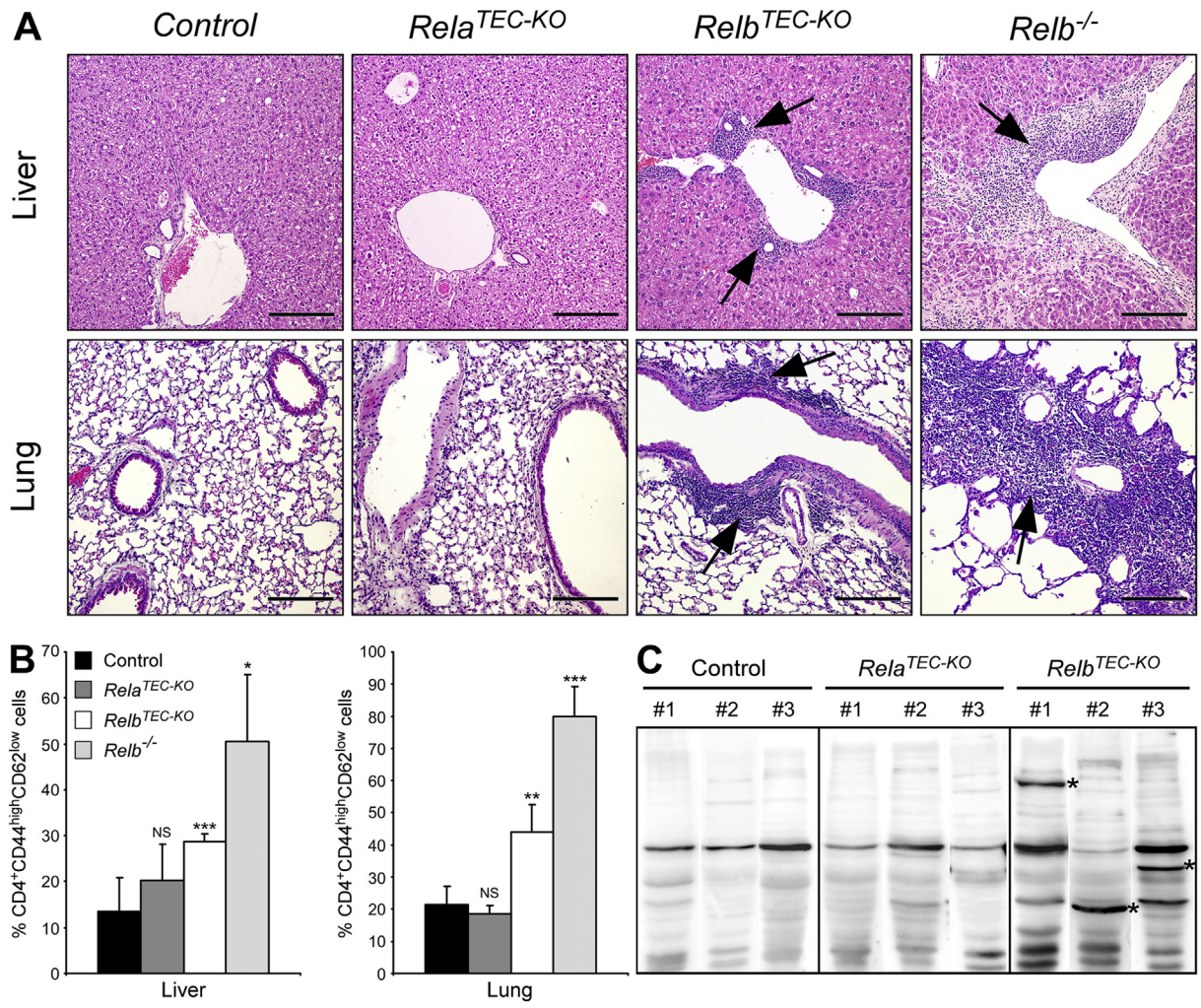

Fig. 3. *Relb*$^{TEC\text{-}KO}$ but not *Rela*$^{TEC\text{-}KO}$ mice develop autoimmunity. (A) Liver and lung sections from 9- to 12-month-old control, *Rela*$^{TEC\text{-}KO}$, *Relb*$^{TEC\text{-}KO}$, and *Relb*$^{-/-}$ mice were stained with H&E. Scale bars represent 200 μm. (B) Frequencies of activated/memory (CD44^{high}CD62^{low}) cells among CD4^{+} T cells in liver (li) and lung (lu) of 4-week-old control (n(li) = 12; n(lu) = 13), *Rela*$^{TEC\text{-}KO}$ (n(li) = 5; n(lu) = 5), *Relb*$^{TEC\text{-}KO}$ (n(li) = 4; n(lu) = 4), and *Relb*$^{-/-}$ (n(li) = 4; n(lu) = 4) mice. Data represent mean values ± SD. (C) *Relb*$^{TEC\text{-}KO}$ but not *Rela*$^{TEC\text{-}KO}$ mice produce autoantibodies. Western blots of liver protein extracts from *Rag1*$^{-/-}$ mice were incubated with serum from three mice per genotype. Asterisks mark protein bands recognized only by sera from *Relb*$^{TEC\text{-}KO}$ mice indicating the presence of autoantibodies.

which was more pronounced in *Relb*$^{TEC\text{-}KO}$ animals (Fig. 2D). Notably, thymic *i*NKT cells were almost completely absent in both *Rela*$^{TEC\text{-}KO}$ and *Relb*$^{TEC\text{-}KO}$ mice. Thus, while mTECs were dispensable for the development of normal numbers of αβ and γδ T cells, they were required for the generation of FoxP3^{+} nTreg and *i*NKT cell populations.

3.3. *Relb*$^{TEC-KO}$ but not *Rela*$^{TEC-KO}$ mice develop autoimmunity

Histopathological examination of multiple tissues from *Relb*$^{TEC\text{-}KO}$ mice showed inflammatory cells preferentially infiltrating liver and lung (Fig. 3A). Flow cytometric analysis furthermore revealed increased frequencies of activated/memory CD4^{+}CD44^{high}CD62^{low} T cells in both tissues of *Relb*$^{TEC\text{-}KO}$ mice, indicating an on-going autoimmune response (Fig. 3B). Moreover, sera from *Relb*$^{TEC\text{-}KO}$ mice reacted against liver proteins of RAG1$^{-/-}$ mice indicating the presence of autoantibodies, another hallmark of autoimmunity (Fig. 3C). However, the autoimmune phenotype in *Relb*$^{TEC\text{-}KO}$ mice was milder than in systemic *Relb*$^{-/-}$ mice, which displayed more severe inflammatory infiltrates (Fig. 3A). Frequencies of activated T cells in infiltrated tissues were also significantly higher in *Relb*$^{-/-}$ compared to age-matched *Relb*$^{TEC\text{-}KO}$ mice (Fig. 3B). These results showed that RelB is essential in mTECs, but is also important in other cell types to establish full self-tolerance. In contrast to *Relb*$^{TEC\text{-}KO}$ mice, *Rela*$^{TEC\text{-}KO}$ mice neither showed autoimmune infiltrates nor autoantibodies (Fig. 3A, B and C). Thus, low levels of thymic PTA expression in combination with only moderately reduced Sirpα^{-} DCs were sufficient to establish self-tolerance in *Rela*$^{TEC\text{-}KO}$ mice.

3.4. RelA controls the number of differentiating mTECs by regulating the expression of RelB

The ubiquitin-ligase Traf6, which can activate the classical NF-κB pathway, has been shown to be essential for the differentiation of mTECs, possibly via induction of RelB expression [38]. To investigate the molecular function of RelA in mTEC differentiation, we compared *Relb* and *Nfkb2* mRNA levels in mTECs, which were sorted by FACS from *Rela*$^{TEC\text{-}KO}$ and control mice (Supplemental Fig. 7). Whereas *Nfkb2* expression was unaltered, expression of the *Relb* gene was reduced in mTECs from *Rela*$^{TEC\text{-}KO}$ mice (Fig. 4A). Interestingly, we observed that thymi from heterozygous *Relb*$^{TEC\text{-}KO}$ mice, harboring only one functional *Relb* allele, contained half the

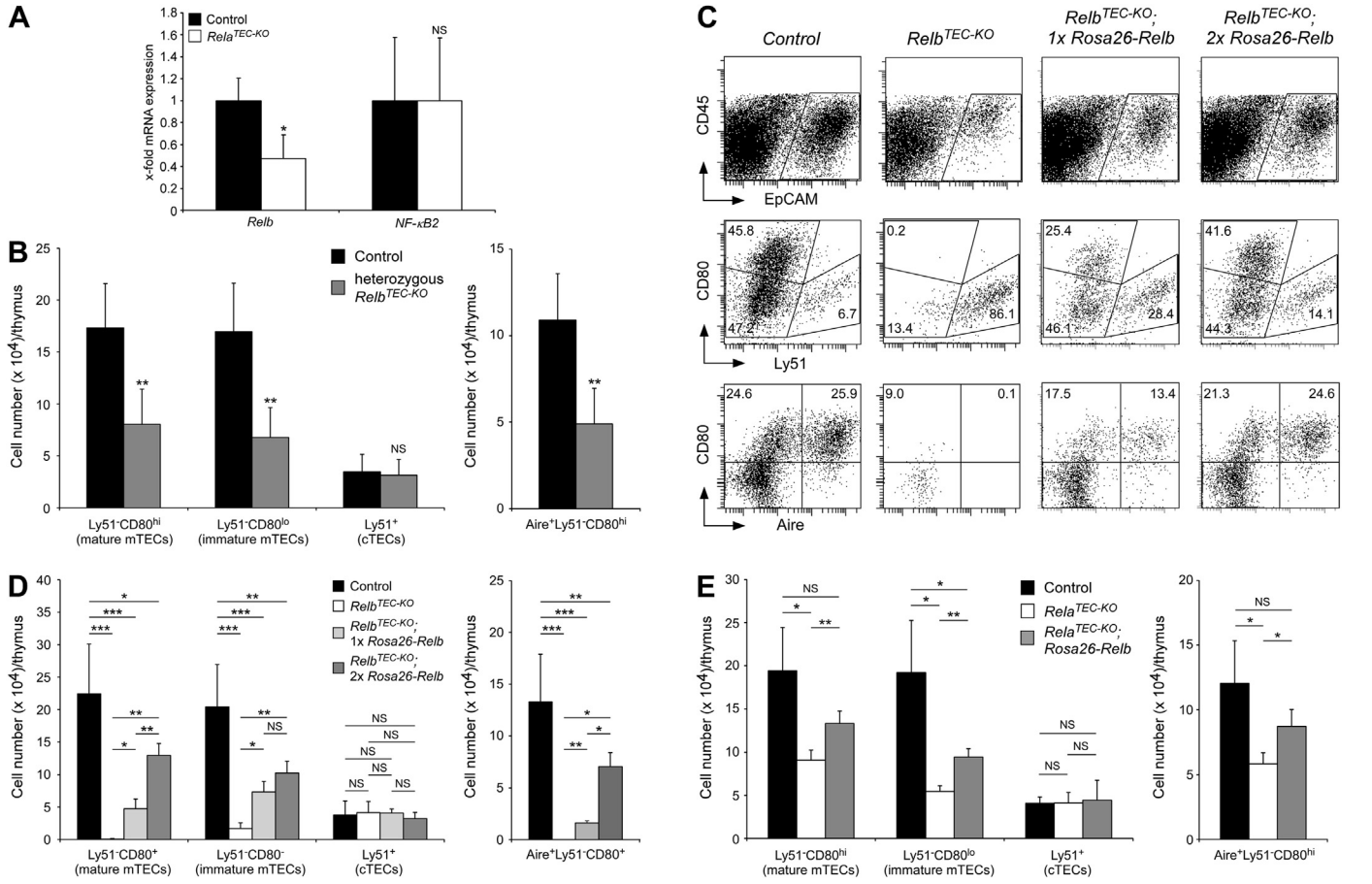

Fig. 4. RelA controls the numbers of differentiating mTECs by regulating the expression of RelB. (A) FACS-purified mTECs from control and *Rela*$^{TEC\text{-}KO}$ mice were analyzed for *Relb* and *Nfkb2* mRNA expression by qRT-PCR. Data represent mean values ± SD from four independent experiments relative to controls after normalization to *Actb*. (B) CD45^{-}EpCAM^{+} epithelial cells from control (n = 6) and heterozygous *Relb*$^{TEC\text{-}KO/+}$ (n = 6) mice were classified as described in Fig. 1B and C. Bar diagrams display total cell numbers of respective TEC subpopulations. (C) Thymus single-cell suspensions from control and *Relb*$^{TEC\text{-}KO}$ mice, as well as from *Relb*$^{TEC\text{-}KO}$ mice with expression of one or two alleles of a *Rosa26-Relb* transgene, were analyzed by flow cytometry as indicated. Numbers in the respective gates show frequencies of TEC subpopulations. (D) Quantitative summary of total cell numbers within the different TEC subpopulations per thymus from control (n = 8) and *Relb*$^{TEC\text{-}KO}$ (n = 5) mice, as well as from *Relb*$^{TEC\text{-}KO}$ mice with expression of one (n = 3) or two (n = 3) alleles of a *Rosa26-Relb* transgene. (E) Thymus cells from control (n = 4) and *Rela*$^{TEC\text{-}KO}$ (n = 3) mice, as well as from *Rela*$^{TEC\text{-}KO}$ mice expressing two alleles of a *Rosa26-Relb* transgene (n = 4) were analyzed as described in (D). Data in (D) and (E) represent mean values ± SD.

number of mTECs compared with control mice, suggesting a direct relationship between RelB dose and the number of differentiating mTECs (Fig. 4B). This notion we tested by expressing either one or two copies of a *Relb* transgene specifically in the thymic epithelium of *Relb*$^{TEC\text{-}KO}$ mice. Therefore, we generated *Rosa26-Relb* mice, which expressed a *Relb* transgene from the *Rosa26* locus in a Cre-dependent manner. These mice were crossed with *Relb*$^{TEC\text{-}KO}$ mice to obtain *Relb*$^{TEC\text{-}KO}$*;Rosa26-Relb* mice with either one or two *Rosa26-Relb* alleles. Importantly, TEC-specific expression of only one allele of the *Relb* transgene was sufficient to release the block in differentiation of mature Aire^{+} mTECs in *Relb*$^{TEC\text{-}KO}$ mice (Fig. 4C and D). The finding that expression of an additional *Relb* transgene allele almost doubled the number of immature and mature mTECs confirmed the assumption that RelB regulates the number of mTECs in a dose-dependent manner.

To genetically investigate whether reduced mTEC differentiation in *Rela*$^{TEC\text{-}KO}$ mice was due to reduced RelB levels, we also expressed two alleles of the *Relb* transgene specifically in RelA-deficient TECs. Transgenic expression of RelB led to a marked restoration of both immature and mature mTEC numbers in *Rela*$^{TEC\text{-}KO}$*;Rosa26-Relb* animals (Fig. 4E). Thus, normal differentiation of mTECs was dependent on the dose of RelB and transcriptional upregulation of RelB via activation of RelA represented a function of the classical NF-κB pathway in mTECs. However, *Relb*$^{TEC\text{-}KO}$ mice completely lacked mTECs while *Rela*$^{TEC\text{-}KO}$ mice had only reduced numbers still expressing detectable levels of RelB. This indicated that besides RelA another transcription factor must be involved in the regulation of RelB in mTECs.

3.5. c-Rel partially compensates for the loss of RelA in transcriptional regulation of RelB expression and mTEC development

Since we found that expression of the NF-κB subunit c-Rel is upregulated in a subpopulation of mature mTECs (Supplemental Fig. 8), it was tempting to speculate that RelA and c-Rel cooperate in the regulation of *Relb*. To reveal a potential role of c-Rel in mTEC development mice with TEC-specific deletion of either the *c-Rel* gene alone (*c-Rel*$^{TEC\text{-}KO}$) or in combination with deletion of the *Rela* gene (*Rela;c-Rel*$^{TEC\text{-}DKO}$) were generated. The thymic epithelia from both mouse lines were analyzed by FACS in parallel with *Rela*$^{TEC\text{-}KO}$ and control thymi. While mTEC numbers in *c-Rel*$^{TEC\text{-}KO}$ mice were not significantly altered compared to controls, the *Rela;c-Rel*$^{TEC\text{-}DKO}$ mice showed a striking reduction of mature and immature mTEC numbers, which was much stronger than in the *Rela*$^{TEC\text{-}KO}$ mice (Fig. 5A). *Rela;c-Rel*$^{TEC\text{-}DKO}$ animals had only few Aire^{+} mature mTECs but did not show any signs of spontaneous autoimmunity

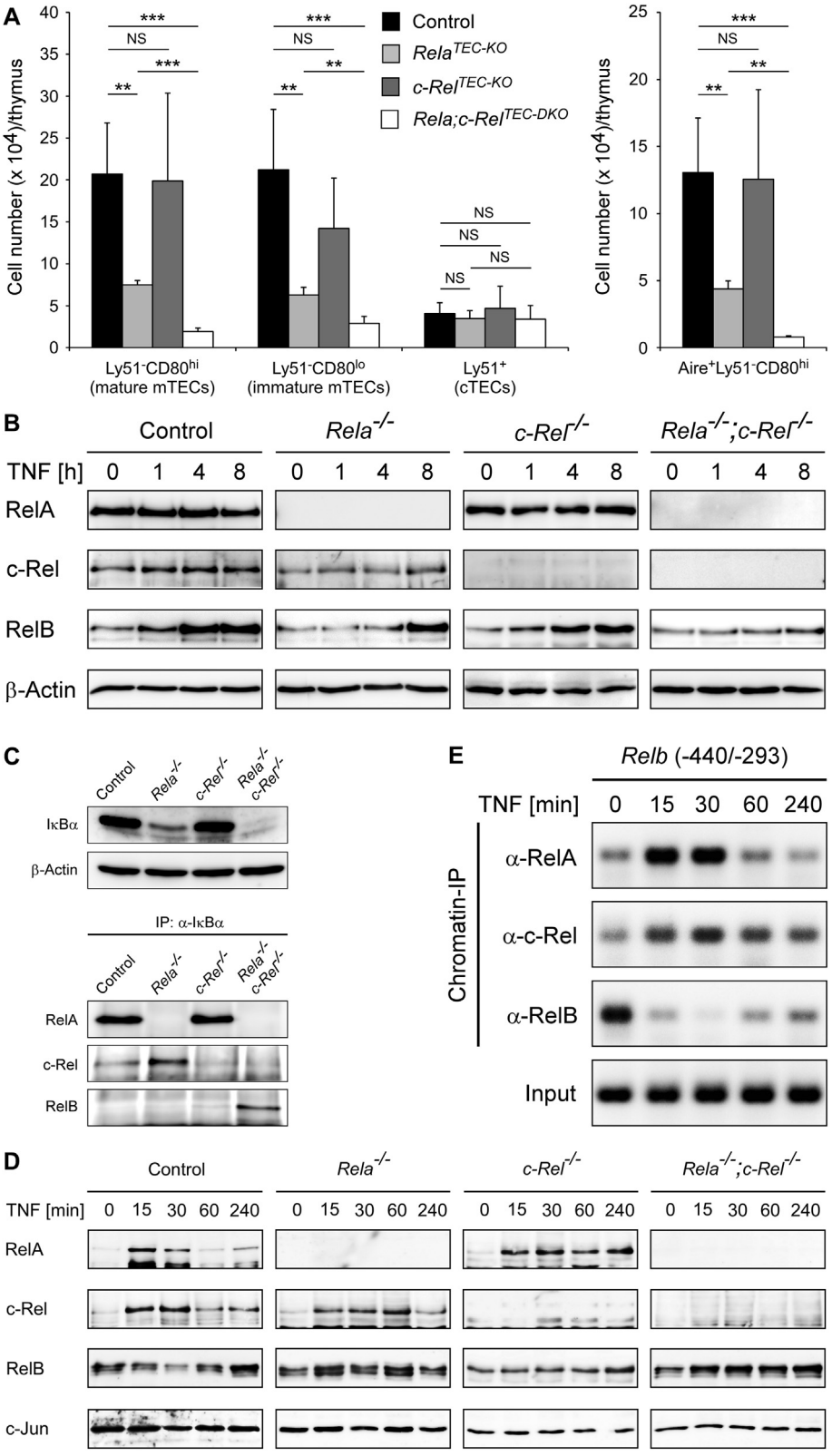

Fig. 5. c-Rel partially compensates the loss of RelA in transcriptional regulation of RelB expression and mTEC development. (A) CD45$^-$EpCAM$^+$ epithelial cells from control (n = 7), *Rela*$^{TEC\text{-}KO}$ (n = 3), *c-Rel*$^{TEC\text{-}KO}$ (n = 4), and *Rela;c-Rel*$^{TEC\text{-}DKO}$ (n = 4) mice were classified into immature, mature, and Aire$^+$ mTECs as well as cTECs as described in Fig. 1B and C. Bar diagrams display total cell numbers of respective TEC subpopulations per thymus and represent mean values ± SD. (B) Induction of RelB protein in MEFs of the indicated genotypes after stimulation with TNF (10 ng/ml). Whole-cell protein extracts were prepared at the times indicated and analyzed by Western blot analysis with antibodies specific for RelA, c-Rel, RelB and β-actin. (C) Interaction of RelA, c-Rel and RelB with IκBα in unstimulated MEFs of the indicated genotypes. (Upper panel) Western blot analysis was performed with whole-cell protein extracts using antibodies specific for IκBα and β-actin. (Lower panel) Whole cell protein extracts were incubated with α-IκBα antibody-coated agarose beads and co-immunoprecipitated proteins RelA, c-Rel and RelB were detected by Western blot analysis. (D) Activation of NF-κB subunits RelA, c-Rel, and RelB in MEFs of the indicated genotypes. Nuclear protein extracts were prepared at different timepoints after stimulation with TNF (10 ng/ml) and analyzed by Western blot analysis with the indicated antibodies. (E) ChIP experiments were performed with 5 μg chromatin of wild-type MEFs at the indicated times after stimulation with TNF (10 ng/ml) using antibodies specific for RelA, c-Rel and RelB. Precipitated DNA was analyzed by PCR using primers encompassing the indicated position in the *Relb* promoter. PCR was also performed with 10 ng of input chromatin to ensure equal loading. In (B), (C), (D) and (E) representative figures from three experimental replicates are shown.

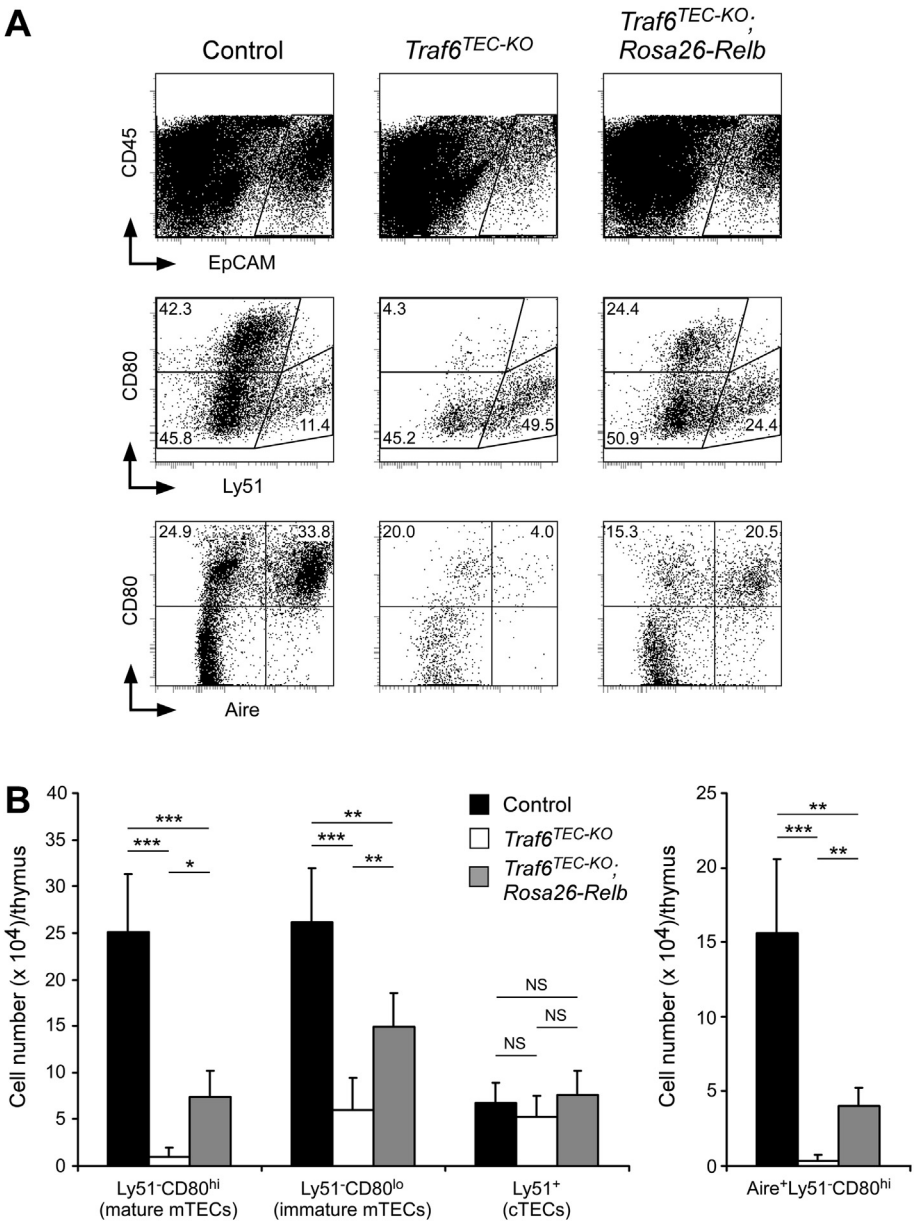

Fig. 6. Traf6 regulates expression of RelB in mTECs. (A) Thymus single-cell suspensions from control and *Traf6*$^{TEC\text{-}KO}$, as well as from *Traf6*$^{TEC\text{-}KO}$ mice expressing two alleles of a *Rosa26-Relb* transgene were stained and analyzed as described in Fig. 1B. (B) Bar diagrams display total cell numbers of respective TEC subpopulations per thymus from control (n = 7) and *Traf6*$^{TEC\text{-}KO}$ (n = 6), as well as from *Traf6*$^{TEC\text{-}KO}$ mice expressing two alleles of a *Rosa26-Relb* transgene (n = 4) and represent mean values ± SD.

such as inflammatory infiltrations in the liver, indicating that even these few mTECs were sufficient to establish central tolerance. Nevertheless, *Rela;c-Rel*$^{TEC\text{-}DKO}$ mice showed a very similar defect in mTEC development as *Relb*$^{TEC\text{-}KO}$ mice. This finding suggested that RelA and c-Rel regulate differentiation of mTECs by cooperatively controlling the expression of RelB. RelA and c-Rel are both activated via the classical NF-κB signaling pathway. To investigate the respective contribution of both factors to the induction of RelB we stimulated 3T3 mouse embryonic fibroblasts (MEF) from wild-type, *Rela*$^{-/-}$, *c-Rel*$^{-/-}$ and *Rela*$^{-/-}$;*c-Rel*$^{-/-}$ mice with TNF, which induces classical but not alternative NF-κB signaling, and measured RelB induction by Western Blot analysis. In wild-type cells, TNF strongly increased RelB protein levels starting at 1 h with further increase at 4 and 8 h after stimulation (Fig. 5B). Compared to wild-type cells, RelB induction was slower but not much weaker in *Rela*$^{-/-}$ and unchanged in *c-Rel*$^{-/-}$ cells. Interestingly, in cells lacking both RelA and c-Rel, RelB levels were only slightly upregulated by TNF, indicating that RelA and c-Rel regulate RelB expression in a redundant but pivotal manner.

In unstimulated cells RelA is complexed with the NF-κB inhibitor IκBα, which is degraded upon induction of the classical NF-κB pathway releasing RelA for nuclear translocation and target gene regulation [17]. To analyze alterations in the NF-κB/IκBα complex in the absence of RelA and/or c-Rel an IκBα-Western-blot as well as IκBα-immunoprecipitations were performed using whole cell extracts from the unstimulated wild-type and mutant MEFs. The co-immunoprecipitated NF-κB subunits RelA, c-Rel and RelB were analyzed by Western blot. While in wild-type and *c-Rel*$^{-/-}$ cells IκBα was mainly complexed with RelA, the depletion of RelA caused a reduction in IκBα protein levels but an increased recruitment of c-Rel into the IκBα-complex (Fig. 5C). In the absence of both RelA and c-Rel the IκBα-protein amount decreased strongly. Interestingly,

the few remaining IκBα was complexed to RelB. To examine the consequences of the alterations in the composition of the IκBα-complex for the activation of the three Rel-proteins by classical NF-κB signaling in the wild-type and mutant MEFs, we analyzed their nuclear translocation after stimulation with TNF. While low levels of RelB protein were constitutively present in the nucleus of control cells RelA and c-Rel rapidly and only shortly translocated into the nucleus after TNF stimulation of wild-type cells (Fig. 5D). The activation of c-Rel in *Rela*$^{-/-}$ cells and of RelA in *c-rel*$^{-/-}$ cells was intact with even prolonged nuclear translocation of both factors. Interestingly, due to the interaction of RelB with IκBα, classical NF-κB signaling induced a quick and sustained activation of RelB in *Rela*$^{-/-}$*;c-Rel*$^{-/-}$ cells. This activation might be responsible for the slight RelB induction in *Rela*$^{-/-}$*;c-Rel*$^{-/-}$ cells (Fig. 5B). Such an autoregulation of the *Relb* gene could also be the reason for the finding that, in contrast to *Relb*$^{TEC\text{-}KO}$ mice, thymi from *Rela;c-Rel*$^{TEC\text{-}DKO}$ mice still had few mature mTECs (Fig. 5A). Since the *Relb* promoter contains three potential NF-κB recognition motifs, we investigated whether RelA, c-Rel and RelB regulate the transcription of RelB by direct binding to its promoter. Chromatin-immunoprecipitations (ChIP) were performed using wild-type cells. Interestingly, we found that in unstimulated cells the *Relb* promoter is occupied with RelB protein itself (Fig. 5E). However, only 15 min after stimulation with TNF it is replaced by RelA and c-Rel. While RelA is dissociated from the *Relb* promoter already after 60 min, the interaction of c-Rel is longer lasting and still present after 240 min. Together, these results clearly show that all three Rel proteins are able to interact with the *Relb* promoter and directly control the transcription of *Relb*.

3.6. *Traf6 regulates expression of RelB in mTECs*

Similar to *Rela;c-Rel*$^{TEC\text{-}DKO}$ and *Relb*$^{TEC\text{-}KO}$ mice, *Traf6*$^{TEC\text{-}KO}$ mice have recently been shown to lack mature mTECs [27]. Since Traf6 transduces the stimulation of RANK and CD40 to classical NF-κB signaling but also to several other pathways [28], we investigated whether loss of mTECs in *Traf6*$^{TEC\text{-}KO}$ mice was also due to inefficient induction of RelB expression. For this, we bred *Traf6*$^{TEC\text{-}KO}$*;Rosa26-Relb* mice and compared their mTEC numbers with those from *Traf6*$^{TEC\text{-}KO}$ mice. Expression of two *Relb* transgene alleles resulted in a clear increase in the numbers of immature and mature mTECs compared to the *Traf6*$^{TEC\text{-}KO}$ mice, verifying that Traf6 controls mTEC development via induction of RelB (Fig. 6A and B). However, this rescue in mTEC numbers by the *Relb* transgene was less efficient in *Traf6*$^{TEC\text{-}KO}$ mice than in *Relb*$^{TEC\text{-}KO}$ mice (Figs. 6B and 4D). This indicates that Traf6 not only activates expression of RelB, but in addition at least one other unknown factor, which plays a RelB-independent role in mTEC development. Since Traf6 mediates the signals from RANK and CD40, we conclude that one important function of both receptors on mTECs is to upregulate the expression of RelB via the classical NF-κB pathway.

3.7. *High NF-κB activity and RelB expression in the majority of mature mTECs*

Our data showed that the transcriptional regulation of RelB by RelA and c-Rel is essential for the differentiation of both immature and mature mTECs. To find out at which stage of mTEC differentiation classical NF-κB signaling induces the expression of RelB, we analyzed two reporter mouse lines, (1) *κB-EGFP* mice, which express EGFP under control of three copies of the NF-κB binding site from the immunoglobulin kappa light chain enhancer, (2) *Relb-Cre-P2A-Katushka* mice, a BAC transgenic mouse line, in which expression of the red fluorescence protein Katushka is regulated by the endogenous regulatory sequences of the *Relb* gene. Flow cytometric analysis of mTECs from *κB-EGFP* mice showed the highest NF-κB activity in the majority of CD80^{hi} mature mTECs, whereas a couple of immature mTECs displayed low basal NF-κB activity (Fig. 7A). Similarly, RelB expression was also mainly confined to CD80^{hi} mature mTECs with low expression in some immature cells (Fig. 7B). This overlap of NF-κB activity and RelB expression not only corroborates the link between both events in mature mTECs, but also indicates that RANK-, CD40-, and LTβR-induced signaling occurs predominantly in these cells.

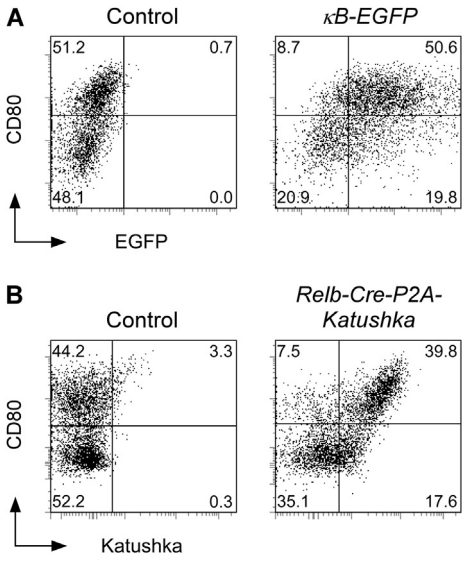

Fig. 7. High NF-κB activity and RelB expression in the majority of mature mTECs. (A) Thymus single-cell suspensions from control and *κB-EGFP* mice were stained and expression of the NF-κB-driven *κB-EGFP* reporter-gene within the CD80^{lo} (immature) and CD80^{hi} (mature) CD45^{-}EpCAM^{+}Ly51^{-} mTECs was analyzed by FACS. (B) CD80^{lo} (immature) and CD80^{hi} (mature) CD45^{-}EpCAM^{+}Ly51^{-} mTECs from control and *Relb-Cre-P2A-Katushka* mice were analyzed by FACS for the *Relb*-promoter driven marker Katushka. (A and B) Numbers in the respective gates indicate frequencies of cells within each mTEC subpopulation. A representative figure from three independent experimental replicates is shown.

4. Discussion

While the importance of alternative NF-κB signaling in differentiation of mature mTECs and in induction of self-tolerance has been well characterized by the analysis of mice with systemic inactivation of its components [19–24], the mTEC-intrinsic role of this pathway as well as the function of the classical NF-κB signaling pathway in both processes is less clear. Here, we used TEC-specific inactivation of NF-κB transcription factors RelA, c-Rel and RelB to delineate and compare the respective contributions of both pathways to these issues. We found that *Relb*$^{TEC\text{-}KO}$ mice lacked all mature mTECs, verifying the cell-intrinsic role of alternative NF-κB signaling in mTEC development. Surprisingly, these mice developed only mild autoimmunity compared to systemic *Relb*$^{-/-}$ mice, indicating that RelB is important in other cell-types, which act together with mTECs to prevent autoimmunity. Indeed *Relb*$^{-/-}$ mice have additional defects in stromal cells of secondary lymphoid organs [25]. These tissues also maintain self-tolerance either through ectopic PTA expression and presentation by stromal cells or through presentation of tissue-derived antigens by immature DCs [39]. In addition, RelB is intrinsically required for proper development and function of DCs [26,40,41]. It was reported that injection of RelB-proficient DCs can ameliorate the severe inflammation of *Relb*$^{-/-}$ mice [26]. The similar inflammatory phenotypes of *Traf6*$^{TEC\text{-}KO}$ and *Relb*$^{TEC\text{-}KO}$ mice further corroborate that specific

depletion of mTECs alone elicits mild autoimmunity affecting predominantly only liver and lung [27].

The selective depletion of all mature and most immature mTECs by TEC-specific ablation of *Relb* makes $Relb^{TEC\text{-}KO}$ mice an ideal tool to investigate the distinct roles these cells play in the thymus. Differentiation of nTregs in thymus can be induced by the presentation of self-antigen on mTECs or DCs [4,6]. However, DCs are not essential for the differentiation of nTregs in thymus since depletion of DCs does not lead to decreased nTreg numbers [42]. In contrast to DCs, mTECs were required for the generation of a normal $FoxP3^+$ nTreg population. However, significant numbers of nTregs still developed in the absence of mTECs in $Relb^{TEC\text{-}KO}$ thymi. One possible explanation for this might be that in the absence of mTECs DCs have taken over their function to drive nTreg differentiation. Notably, $SIRP\alpha^+$ cDCs, which have been shown to be the most potent DC subpopulation for nTreg instruction [4], were not affected in $Relb^{TEC\text{-}KO}$ mice, while $CD8^+SIRP\alpha^-$ cDCs, which were reduced in $Relb^{TEC\text{-}KO}$ mice, have very recently been shown to be dispensable for nTreg induction [43].

The strong reduction of mTECs in $Rela;c\text{-}Rel^{TEC\text{-}DKO}$ mice demonstrates that classical NF-κB signaling plays a cell-intrinsic role in mTEC development, which seems to be as important as the alternative NF-κB pathway. The finding that $Rela;c\text{-}Rel^{TEC\text{-}DKO}$ mice still contained few mature mTECs and didn't develop spontaneous autoimmunity might be due to the compensation of the RelA and c-Rel function in classical NF-κB signaling by RelB. This is supported by the finding that RelB is recruited into a complex with IκBα in $Rela^{-/-};c\text{-}Rel^{-/-}$ MEFs, rendering it inducible by classical NF-κB signaling after TNF stimulation. A similar mechanism was previously described for DCs, in which strong upregulation of RelB during maturation elicited its incorporation into an IκBα-complex [41].

Since ablation of RelA resulted in decreased *Relb* mRNA levels in a diminished number of mTECs, which could be partly rescued by TEC-specific expression of a *Relb* transgene, our data show that one main function of classical NF-κB signaling in mTECs is to upregulate the expression of RelB. The experiments with TNF-stimulated MEFs further show that this crosstalk between classical and alternative NF-κB signaling is based on a direct transcriptional regulation of RelB by RelA and c-Rel and probably also underlies the overlapping roles of RelA and c-Rel in mTEC development.

Classical NF-κB signaling is one pathway among others that can be activated by several receptors via the ubiquitin ligase Traf6 [28]. Traf6 has been shown to be essential for mTEC development [27,38], however the involved downstream signaling pathways were not clear. Our finding that the block in mTEC development due to Traf6-deficiency can be overcome by expression of a *Relb* transgene indicates that RelB upregulation by RelA and c-Rel acts downstream of Traf6 in mTECs. However, this does not exclude that other Traf6-dependent pathways as well might play a role. This is suggested by the less efficient rescue of mature mTEC numbers by *Relb* transgene expression in $Traf6^{TEC\text{-}KO}$ compared to $Relb^{TEC\text{-}KO}$ mice. For instance, IRF7, which can be activated by Traf6 [28], has recently been reported to be important for mTEC development [44].

Interestingly, a recent publication showed that activation of alternative NF-κB signaling in mTECs by inactivation of Traf3 could completely revert the strong decrease of mTEC numbers in $Cd40^{-/-};Lt\beta r^{-/-}$ but not in $Rankl^{-/-}$ mice, demonstrating that a pathway distinct from alternative NF-κB signaling is essential for mTEC development downstream of RANK [45]. This suggests that the induction of RelB by RelA and c-Rel downstream of Traf6 is initiated primarily by RANK stimulation on mTECs and that CD40- and LTβR-stimulation contribute secondarily, since mTECs are not completely absent in $Rankl^{-/-}$ mice. Whether RANK is also needed for activation of alternative NF-κB signaling in mTECs remains to be addressed.

We found that activation of NF-κB and high expression of RelB was predominantly confined to $CD80^{hi}$ mature mTECs. This was quite surprising taking into consideration that $Relb^{TEC\text{-}KO}$, as well as $Rela;c\text{-}Rel^{TEC\text{-}DKO}$ and $Traf6^{TEC\text{-}KO}$ mice not only loose $CD80^{hi}$ mature mTECs, but also their presumed $CD80^{lo}$ immature progenitors. While RelB is dispensible for the development and maintenance of the mTEC stem cells [46], it cannot be excluded that low RelB levels in $CD80^{lo}$ mTECs are essential for the differentiation of the whole mTEC lineage and high levels of RelB in $CD80^{hi}$ mTECs fulfill an additional and different role. For example, high expression of RelB in mature DCs has been shown to be important for upregulation of the surface proteins CD80, MHC II and CD40 [41], which are also expressed on mature mTECs. However, alternatively, high RelB levels in mature mTECs might be essential for the expression of so far unknown mediators, which directly or indirectly control the differentiation of early progenitors toward the mTEC lineage in a feedback mechanism. One such factor among others might be CCL21, a target gene of alternative NF-κB signaling [17]. It is expressed by mTECs which either directly derive from $Aire^+$ mTECs or are promoted by them in their development [47]. CCL21 is involved in medulla recruitment of positively selected thymocytes, which have been shown to also induce differentiation of mTECs [13,48]. Furthermore, the findings that CCL21-expressing mTECs as well as terminally differentiated involucrin$^+$ $Aire^-$ mTECs, which also derive from $Aire^+$ mature cells, have low expression of CD80, suggest that a proportion of $CD80^{lo}$ mTECs rather derive from $CD80^{hi}$ mature mTECs than being their predecessors [11,47]. Thus, the loss of at least some $CD80^{lo}$ cells in our mutant mice might be due to a developmental block at the $CD80^{hi}$ mature mTEC stage.

Collectively, our findings reveal an mTEC-intrinsic role for classical NF-κB signaling in establishment of self-tolerance. Its crosstalk with alternative NF-κB signaling by inducing the expression of RelB turned out to be essential for development of mature mTECs. We showed that these were important for PTA expression, nTreg induction, *i*NKT cell development and presence of $Sirp\alpha^+$ migratory DC in thymus and for prevention of autoimmunity in peripheral organs.

Author contributions

M.R. and F.W. conceived of the project; M.R., N.A., M.F., E.M., D.W., H.F. and F.W. designed and performed the research and analyzed and interpreted the data; R.S.-U., U.K. and Z.-Q.W. facilitated the research; M.R. prepared the figures and wrote the manuscript.

Disclosures

The authors have no financial conflicts of interest.

Acknowledgements

We gratefully acknowledge A. Gompf for excellent technical assistance and R. Hänold for reading the manuscript. We thank H. Rosemann and D. Galendo in the animal facility of the FLI. We are indebted to T. Böhm for *FoxN1-Cre*, R.M. Schmid for $Rela^{flox}$ and M. Pasparakis for $Traf6^{flox}$ mice as well as U. Zimber-Strobl for plasmids and M. Schmidt-Supprian and A. Hoffmann for mutant mouse embryonic 3T3 fibroblasts. This work was supported by grants from the Deutsche Forschungsgemeinschaft (grants WE 2224/6 and WE 2224/6-2 to M.R. and F.W.). Funding for open access charge: Leibniz Institute on Aging, Fritz Lipmann Institute (FLI), Jena, Germany. The FLI is a member of the Leibniz Association and is financially

supported by the Federal Government of Germany and the State of Thuringia.

Appendix A. Supplementary data

Supplementary data related to this article can be found at http://dx.doi.org/10.1016/j.jaut.2017.03.007.

References

[1] G. Anderson, S. Baik, J.E. Cowan, A.M. Holland, N.I. McCarthy, K. Nakamura, et al., Mechanisms of thymus medulla development and function, Curr. Top. Microbiol. Immunol. 373 (2014) 19–47.

[2] J. Derbinski, A. Schulte, B. Kyewski, L. Klein, Promiscuous gene expression in medullary thymic epithelial cells mirrors the peripheral self, Nat. Immunol. 2 (2001) 1032–1039.

[3] M.S. Anderson, E.S. Venanzi, L. Klein, Z. Chen, S.P. Berzins, S.J. Turley, et al., Projection of an immunological self shadow within the thymus by the Aire protein, Science 298 (2002) 1395–1401.

[4] A.I. Proietto, S. van Dommelen, P. Zhou, A. Rizzitelli, A. D'Amico, R.J. Steptoe, et al., Dendritic cells in the thymus contribute to T-regulatory cell induction, Proc. Natl. Acad. Sci. U. S. A. 105 (2008) 19869–19874.

[5] J. Li, J. Park, D. Foss, I. Goldschneider, Thymus-homing peripheral dendritic cells constitute two of the three major subsets of dendritic cells in the steady-state thymus, J. Exp. Med. 206 (2009) 607–622.

[6] J.S. Perry, C.W. Lio, A.L. Kau, K. Nutsch, Z. Yang, J.I. Gordon, et al., Distinct contributions of Aire and antigen-presenting-cell subsets to the generation of self-tolerance in the thymus, Immunity 41 (2014) 414–426.

[7] C.C. Bleul, T. Corbeaux, A. Reuter, P. Fisch, J.S. Mönting, T. Boehm, Formation of a functional thymus initiated by a postnatal epithelial progenitor cell, Nature 441 (2006) 992–996.

[8] S. Baik, E.J. Jenkinson, P.J. Lane, G. Anderson, W.E. Jenkinson, Generation of both cortical and Aire^{+} medullary thymic epithelial compartments from CD205^{+} progenitors, Eur. J. Immunol. 43 (2013) 589–594.

[9] I. Ohigashi, S. Zuklys, M. Sakata, C.E. Mayer, S. Zhanybekova, S. Murata, et al., Aire-expressing thymic medullary epithelial cells originate from β5t-expressing progenitor cells, Proc. Natl. Acad. Sci. U. S. A. 110 (2013) 9885–9890.

[10] M. Sekai, Y. Hamazaki, N. Minato, Medullary thymic epithelial stem cells maintain a functional thymus to ensure lifelong central T cell tolerance, Immunity 41 (2014) 753–761.

[11] A.J. White, K. Nakamura, W.E. Jenkinson, M. Saini, C. Sinclair, B. Seddon, et al., Lymphotoxin signals from positively selected thymocytes regulate the terminal differentiation of medullary thymic epithelial cells, J. Immunol. 185 (2010) 4769–4776.

[12] S.W. Rossi, M.Y. Kim, A. Leibbrandt, S.M. Parnell, W.E. Jenkinson, S.H. Glanville, et al., RANK signals from CD4^{+}3^{-} inducer cells regulate development of Aire-expressing epithelial cells in the thymic medulla, J. Exp. Med. 204 (2007) 1267–1272.

[13] M. Irla, S. Hugues, J. Gill, T. Nitta, Y. Hikosaka, I.R. Williams, et al., Autoantigen-specific interactions with CD4^{+} thymocytes control mature medullary thymic epithelial cell cellularity, Immunity 29 (2008) 451–463.

[14] N.A. Roberts, A.J. White, W.E. Jenkinson, G. Turchinovich, K. Nakamura, D.R. Withers, et al., Rank signaling links the development of invariant γδ T cell progenitors and Aire^{+} medullary epithelium, Immunity 36 (2012) 427–437.

[15] A.J. White, W.E. Jenkinson, J.E. Cowan, S.M. Parnell, A. Bacon, N.D. Jones, et al., An essential role for medullary thymic epithelial cells during the intrathymic development of invariant NKT cells, J. Immunol. 192 (2014) 2659–2666.

[16] T. Boehm, S. Scheu, K. Pfeffer, C.C. Bleul, Thymic medullary epithelial cell differentiation, thymocyte emigration, and the control of autoimmunity require lympho-epithelial cross talk via LTβR, J. Exp. Med. 198 (2003) 757–769.

[17] E. Dejardin, The alternative NF-κB pathway from biochemistry to biology: pitfalls and promises for future drug development, Biochem. Pharmacol 72 (2006) 1161–1179.

[18] T. Akiyama, Y. Shimo, H. Yanai, J. Qin, D. Ohshima, Y. Maruyama, et al., The tumor necrosis factor family receptors RANK and CD40 cooperatively establish the thymic medullary microenvironment and self-tolerance, Immunity 29 (2008) 423–437.

[19] L. Burkly, C. Hession, L. Ogata, C. Reilly, L.A. Marconi, D. Olson, et al., Expression of relB is required for the development of thymic medulla and dendritic cells, Nature 373 (1995) 531–536.

[20] F. Weih, D. Carrasco, S.K. Durham, D.S. Barton, C.A. Rizzo, R.-P. Ryseck, et al., Multiorgan inflammation and hematopoietic abnormalities in mice with a targeted disruption of RelB, a member of the NF-κB/Rel family, Cell 80 (1995) 331–340.

[21] F. Kajiura, S. Sun, T. Nomura, K. Izumi, T. Ueno, Y. Bando, et al., NF-kappa B-inducing kinase establishes self-tolerance in a thymic stroma-dependent manner, J. Immunol. 172 (2004) 2067–2075.

[22] D. Kinoshita, F. Hirota, T. Kaisho, M. Kasai, K. Izumi, Y. Bando, et al., Essential role of IkappaB kinase alpha in thymic organogenesis required for the establishment of self-tolerance, J. Immunol. 176 (2006) 3995–4002.

[23] M. Zhu, R.K. Chin, P.A. Christiansen, J.C. Lo, X. Liu, C. Ware, et al., NF-κB2 is required for the establishment of central tolerance through an Aire-dependent pathway, J. Clin. Invest. 116 (2006) 2964–2971.

[24] X. Zhang, H. Wang, E. Claudio, K. Brown, U. Siebenlist, A role for the IkappaB family member Bcl-3 in the control of central immunologic tolerance, Immunity 27 (2007) 438–452.

[25] F. Weih, J. Caamano, Regulation of secondary lymphoid organ development by the nuclear factor-kappaB signal transduction pathway, Immunol. Rev. 195 (2003) 91–105.

[26] B.J. O'Sullivan, S. Pai, S. Street, X. An, K.P.A. MacDonald, M. Wong, et al., Immunotherapy with costimulatory dendritic cells to control autoimmune inflammation, J. Immunol. 187 (2011) 4018–4030.

[27] A.J. Bonito, C. Aloman, M.I. Fiel, N.M. Danzl, S. Cha, E.G. Weinstein, et al., Medullary thymic epithelial cell depletion leads to autoimmune hepatitis, J. Clin. Invest. 123 (2013) 3510–3524.

[28] M.C. Walsh, J. Lee, Y. Choi, Tumor necrosis factor receptor-associated factor 6 (TRAF6) regulation of development, function, and homeostasis of the immune system, Immunol. Rev. 266 (2015) 72–92.

[29] C. Soza-Ried, C.C. Bleul, M. Schorpp, T. Boehm, Maintenance of thymic epithelial phenotype requires extrinsic signals in mouse and zebrafish, J. Immunol. 181 (2008) 5272–5277.

[30] H. Algül, M. Treiber, M. Lesina, H. Nakhai, D. Saur, F. Geisler, et al., Pancreas-specific RelA/p65 truncation increases susceptibility of acini to inflammation-associated cell death following cerulein pancreatitis, J. Clin. Invest. 117 (2007) 1490–1501.

[31] N. Heise, N.S. De Silva, K. Silva, A. Carette, G. Simonetti, M. Pasparakis, et al., Germinal center B cell maintenance and differentiation are controlled by distinct NF-κB transcription factor subunits, J. Exp. Med. 211 (2014) 2103–2118.

[32] A. Polykratis, G. van Loo, S. Xanthoulea, M. Hellmich, M. Pasparakis, Conditional targeting of tumor necrosis factor receptor-associated factor 6 reveals opposing functions of Toll-like receptor signalling in endothelial and myeloid cells in a mouse model of atherosclerosis, Circulation 126 (2012) 1739–1751.

[33] P. Tomann, R. Paus, S.E. Millar, C. Scheidereit, R. Schmidt-Ullrich, LHX2 is a direct NF-κB target gene that promotes primary hair follicle placode down-growth, Development 143 (2016) 1512–1522.

[34] D. Gray, J. Abramson, C. Benoist, D. Mathis, Proliferative arrest and rapid turnover of thymic epithelial cells expressing Aire, J. Exp. Med. 204 (2007) 2521–2528.

[35] E. Schreiber, P. Matthias, M.M. Müller, W. Schaffner, Rapid detection of octamer binding proteins with 'mini-extracts', prepared from a small number of cells, Nucleic Acids Res. 17 (1989) 6419.

[36] Y. Hamazaki, H. Fujita, T. Kobayashi, Y. Choi, H.S. Scott, M. Matsumoto, et al., Medullary thymic epithelial cells expressing Aire represent a unique lineage derived from cells expressing claudin, Nat. Immunol. 8 (2007) 304–311.

[37] K. Shortman, W.R. Heath, The CD8^{+} dendritic cell subset, Immunol. Rev. 234 (2010) 18–31.

[38] T. Akiyama, S. Maeda, S. Yamane, K. Ogino, M. Kasai, F. Kajiura, et al., Dependence of self-tolerance on TRAF6-directed development of thymic stroma, Science 308 (2005) 248–251.

[39] D. Malhotra, A.L. Fletcher, S.J. Turley, Stromal and hematopoietic cells in secondary lymphoid organs: partners in immunity, Immunol. Rev. 251 (2013) 160–176.

[40] L. Wu, A. D'Amico, K.D. Winkel, M. Suter, D. Lo, K. Shortman, RelB is essential for the development of myeloid-related CD8alpha- dendritic cells but not of lymphoid-related CD8alpha+ dendritic cells, Immunity 9 (1998) 839–847.

[41] V.F. Shih, J. Davis-Turak, M. Macal, J.Q. Huang, J. Ponomarenko, J.D. Kearns, et al., Control of RelB during dendritic cell activation integrates canonical and noncanonical NF-κB pathways, Nat. Immunol. 13 (2012) 1162–1170.

[42] C. Ohnmacht, A. Pullner, S.B. King, I. Drexler, S. Meier, T. Brocker, et al., Constitutive ablation of dendritic cells breaks self-tolerance of CD4 T cells and results in spontaneous fatal autoimmunity, J. Exp. Med. 206 (2009) 549–559.

[43] O. Herbin, A.J. Bonito, S. Jeong, E.G. Weinstein, A.H. Rahman, H. Xiong, et al., Medullary thymic epithelial cells and CD8α^{+} dendritic cells coordinately regulate central tolerance but CD8α^{+} cells are dispensable for thymic regulatory T cell production, J. Autoimmun. 75 (2016) 141–149.

[44] D.C. Otero, D.P. Baker, M. David, IRF7-dependent IFN-β production in response to RANKL promotes medullary thymic epithelial cell development, J. Immunol. 190 (2013) 3289–3298.

[45] S.R. Jenkinson, J.A. Williams, H. Jeon, J. Zhang, T. Nitta, I. Ohigashi, et al., TRAF3 enforces the requirement for T cell cross-talk in thymic medullary epithelial development, Proc. Natl. Acad. Sci. U. S. A. 110 (2013) 21107–21112.

[46] S. Baik, M. Sekai, Y. Hamazaki, W.E. Jenkinson, G. Anderson, Relb acts downstream of medullary thymic epithelial stem cells and is essential for the emergence of RANK(+) medullary epithelial progenitors, Eur. J. Immunol. 46 (2016) 857–862.

[47] E. Lkhagvasuren, M. Sakata, I. Ohigashi, Y. Takahama, Lymphotoxin β receptor regulates the development of CCL21-expressing subset of postnatal medullary thymic epithelial cells, J. Immunol. 190 (2013) 5110–5117.

[48] T. Ueno, F. Saito, D.H. Gray, S. Kuse, K. Hieshima, H. Nakano, et al., CCR7 signals are essential for cortex-medulla migration of developing thymocytes, J. Exp. Med. 200 (2004) 493–505.